

Journal of Visualized Experiments

Chemical Dimerization-Induced Protein Condensates on Telomeres

--Manuscript Draft--

Article Type:	Invited Methods Collection - JoVE Produced Video
Manuscript Number:	JoVE62173R1
Full Title:	Chemical Dimerization-Induced Protein Condensates on Telomeres
Corresponding Author:	Huaiying Zhang Carnegie Mellon University Pittsburgh, PA UNITED STATES
Corresponding Author's Institution:	Carnegie Mellon University
Corresponding Author E-Mail:	huaiyinz@andrew.cmu.edu
Order of Authors:	Rongwei Zhao David Chenoweth Huaying Zhang
Additional Information:	
Question	Response
Please specify the section of the submitted manuscript.	Biology
Please indicate whether this article will be Standard Access or Open Access.	Standard Access (US\$2,400)
Please indicate the city, state/province, and country where this article will be filmed . Please do not use abbreviations.	pittsburgh, Pennsylvania, United States
Please confirm that you have read and agree to the terms and conditions of the author license agreement that applies below:	I agree to the Author License Agreement
Please provide any comments to the journal here.	

TITLE:

Chemical Dimerization-Induced Protein Condensates on Telomeres

AUTHORS AND AFFILIATIONS:

Rongwei Zhao¹, David M. Chenoweth², Huaiying Zhang^{1*}

¹Department of Biological Sciences, Mellon College of Science, Carnegie Mellon University, Pittsburgh, PA, United States

²Department of Chemistry, School of Arts and Sciences, University of Pennsylvania, Philadelphia, PA, United States

Corresponding Author:

Huaiying Zhang (huaiyinz@andrew.cmu.edu)

Email Addresses of Co-authors:

Rongwei Zhao (rongweiz@andrew.cmu.edu)

David M. Chenoweth (dcheno@sas.upenn.edu)

Huaiying Zhang (huaiyinz@andrew.cmu.edu)

KEYWORDS:

condensates, liquid-liquid phase separation, chemical dimerizer, local condensation, telomeres, PML nuclear body

SUMMARY:

This protocol illustrates a chemically induced protein dimerization system to create condensates on chromatin. The formation of promyelocytic leukemia (PML) nuclear body on telomeres with chemical dimerizers is demonstrated. Droplet growth, dissolution, localization, and composition are monitored with live cell imaging, immunofluorescence (IF) and fluorescence in situ hybridization (FISH).

ABSTRACT:

Chromatin-associated condensates are implicated in many nuclear processes, but the underlying mechanisms remain elusive. This protocol describes a chemically induced protein dimerization system to create condensates on telomeres. The chemical dimerizer consists of two linked ligands that can each bind to a protein: Halo ligand to Halo-enzyme and trimethoprim (TMP) to *E. coli* dihydrofolate reductase (eDHFR), respectively. Fusion of Halo enzyme to a telomere protein anchors dimerizers to telomeres through covalent Halo ligand-enzyme binding. Binding of TMP to eDHFR recruits eDHFR-fused phase separating proteins to telomeres and induces condensate formation. Because TMP-eDHFR interaction is non-covalent, condensation can be reversed by using excess free TMP to compete with the dimerizer for eDHFR binding. An example of inducing promyelocytic leukemia (PML) nuclear body formation on telomeres and determining condensate growth, dissolution, localization, and composition is shown. This method can be easily adapted to induce condensates at other genomic locations by fusing Halo to a protein that directly binds to the local chromatin or to dCas9 that is targeted to the genomic locus with a

guide RNA. By offering the temporal resolution required for single cell live imaging while maintaining phase separation in a population of cells for biochemical assays, this method is suitable for probing both the formation and function of chromatin-associated condensates.

INTRODUCTION:

Many proteins and nucleic acids undergo liquid-liquid phase separation (LLPS) and self-assemble into biomolecular condensates to organize biochemistry in cells^{1,2}. LLPS of chromatin-binding proteins leads to the formation of condensates that are associated with specific genomic loci and are implicated in various local chromatin functions³. For example, LLPS of HP1 protein underlies the formation of heterochromatin domains to organize the genome^{4,5}, LLPS of transcription factors forms transcription centers to regulate transcription⁶, LLPS of nascent mRNAs and multi-sex combs protein generates histone locus bodies to regulate the transcription and processing of histone mRNAs⁷. However, despite many examples of chromatin-associated condensates being discovered, the underlying mechanisms of condensate formation, regulation, and function remain poorly understood. In particular, not all chromatin-associated condensates are formed through LLPS and careful evaluations of condensate formation in live cells are still needed^{8,9}. For example, HP1 protein in mouse is shown to have only a weak capacity to form liquid droplets in live cells and heterochromatin foci behave as collapsed polymer globules¹⁰. Therefore, tools to induce de novo condensates on chromatin in living cells are desirable, particularly those that allow the use of live imaging and biochemical assays to monitor the kinetics of condensate formation, the physical and chemical properties of the resulting condensates, and the cellular consequences of condensate formation.

This protocol reports a chemical dimerization system to induce protein condensates on chromatin¹¹ (**Figure 1A**). The dimerizer consists of two linked protein-interacting ligands: trimethoprim (TMP) and Halo ligand and can dimerize proteins fused to the cognate receptors: *Escherichia coli* dihydrofolate reductase (eDHFR) and a bacterial alkyldehalogenase enzyme (Halo enzyme), respectively¹². The interaction between Halo ligand and Halo enzyme is covalent, allowing Halo enzyme to be used as an anchor by fusing it to a chromatin-binding protein to recruit a phase-separating protein fused to eDHFR to chromatin. After the initial recruitment, increased local concentration of the phase separating protein passes the critical concentration needed for phase separation and thus nucleates a condensate at the anchor (**Figure 1B**). By fusing fluorescent proteins (e.g., mCherry and eGFP) to eDHFR and Halo, nucleation and growth of condensates can be visualized in real time with fluorescence microscopy. Because the interaction between eDHFR and TMP is non-covalent, excess free TMP can be added to compete with the dimerizer for eDHFR binding. This will then release the phase separation protein from the anchor and dissolve the chromatin-associated condensate.

We used this tool to induce de novo promyelocytic leukemia (PML) nuclear body formation on telomeres in telomerase-negative cancer cells that use an alternative lengthening (ALT) pathway for telomere maintenance^{13,14}. PML nuclear bodies are membrane-less compartments involved in many nuclear processes^{15,16} and are uniquely localized to ALT telomeres to form APBs, for ALT telomere-associated PML bodies^{17,18}. Telomeres cluster within APBs, presumably to provide repair templates for homology-directed telomere DNA synthesis in ALT¹⁹. Indeed, telomere DNA

synthesis has been detected in APBs, which play essential roles in enriching DNA repair factors on telomeres^{20,21}. However, the mechanisms underlying APB assembly and telomere clustering within APBs were unknown. Since telomere proteins in ALT cells are uniquely modified by small ubiquitin-like modifiers (SUMO)²², many APB components contain sumoylation sites^{22–25} and/or SUMO-interacting motifs (SIMs)^{26,27} and SUMO-SIM interactions drive phase separation²⁸, we hypothesized that sumoylation on telomeres leads to enrichment of SUMO/SIM containing proteins and SUMO-SIM interactions between those proteins lead to phase separation. PML protein, which has three sumoylation sites and one SIM site, can be recruited to form APBs and coalescence of liquid APBs leads to telomeres clustering. To test this hypothesis, we used the chemical dimerization system to mimic sumoylation-induced APB formation by recruiting SIM to telomeres (**Figure 2A**)¹¹. GFP is fused to Haloenzyme for visualization and to the telomere-binding protein TRF1 to anchor the dimerizer to telomeres. SIM is fused to eDHFR and mCherry. Kinetics of condensate formation and droplet fusion-induced telomere clustering is followed with live cell imaging. Phase separation is reversed by adding excess free TMP to compete with eDHFR binding. Immunofluorescence (IF) and fluorescence in situ hybridization (FISH) is used to determine condensate composition and telomeric association. Recruiting SIM enriches SUMO on telomeres and the induced condensates contain PML and therefore are APBs. Recruiting a SIM mutant that cannot interact with SUMO does not enrich SUMO on telomeres or induce phase separation, indicating that the fundamental driving force for APB condensation is SUMO-SIM interaction. Agreeing with this observation, polySUMO-polySIM polymers that fused to a TRF2 binding factor RAP1 can also induce APB formation²⁹. Compared to the polySUMO-polySIM fusion system where phase separation occurs as long as enough proteins are produced, the chemical dimerization approach presented here induces phase separation on demand and thus offers better temporal resolution to monitor the kinetics of phase separation and telomere clustering process. In addition, this chemical dimerization system permits the recruitment of other proteins to assess their ability in inducing phase separation and telomere clustering. For example, a disordered protein recruited to telomeres can also form droplets and cluster telomeres without inducing APB formation, suggesting telomere clustering is independent of APB chemistry and only relies on APB liquid property¹¹.

PROTOCOLS:

1. Production of transient cell lines

1.1. Culture U2OS acceptor cells on 22 x 22 mm glass coverslips (for live imaging) or 12 mm diameter circular coverslips (for IF or FISH) coated with poly-D-lysine in 6-well plate with growth medium (10% fetal bovine serum in DMEM) until they reach 60%–70% confluency.

1.2. Replace the growth medium with 1 mL of transfection medium (growth medium without fetal bovine serum) prior to transfection.

1.3. For each transfection well, add 4 μ L of transfection reagent to 150 μ L of reduced serum media, vortex for 10 s and then incubate for 5 min.

1.4. For each well, add Halo construct plasmid (Halo-GFP-TRF1 or Halo-TRF1) and eDHFR construct plasmid (mCherry-eDHFR-SIM or mCherry-eDHFR-SIM mutant) at a 1:1 mass ratio (0.5 µg Halo construct plasmid with 0.5 µg eDHFR construct plasmid) to 150 µL reduced serum media, dropwise, mix by pipetting.

NOTE: The tags are relatively small (Halo 33 kD, eDHFR 28 kD, mCherry 30 kD, eGFP 27 kD) and no effect on phase separation was observed. However, using mutants such as SIM mutant used here to make sure that the phase behavior is sensitive to the mutations not the tags is advised. SIM is from PIASx^{28,30}. SIM sequence is AAAGTCGATGTAATTGACTTAACGATCGAATCTAGCAGCGATGAAGAAGAAGATCCACCGGCTAAACGT. SIM mutant is generated by mutating SIM amino acids VIDL to VADA²⁸, and the sequence is AAAGTCGATGTAGCCGACGCCACGATCGAATCTAGCAGCGATGAAGAAGAAGATCCACCGGCTAAACGT.

1.5. Add 150 µL of transfection reagent -reduced serum media mixture to 150 µL of reduced serum media with DNA, dropwise, mix by pipetting, incubate for 5 min.

1.6. Add 300 µL of DNA mixture to cells, dropwise and then place cells back into the incubator.

1.7. Wait 24–48 h before live imaging, immunofluorescence (IF) or fluorescence in situ hybridization (FISH).

2. Dimerization on telomeres

2.1. Dissolve dimerizers in DMSO at 10 mM and store in plastic microcentrifuge tubes at –80 °C for long-term storage.

NOTE: Instead of using the dimerizer with TMP directly linked to Halo (TMP-Halo, TH), dimerizer TMP-NVOC-Halo (TNH) that has a photosensitive linker, 6-nitroveratryl oxycarbonyl (NVOC), between TMP and Haloligand is used³¹. This is because it takes less time for TNH (~5 min) to diffuse into the cell than TH (~20 min). Results shown here can also be obtained using TH. When using TNH, be careful not to expose the dimerizer to light to avoid NOVC cleavage. Handle TNH in a dark room with a dim red-light lamp, store the dimerizer in amber plastic tubes and wrap the container containing TNH or treated cells with aluminum foil. Imaging TNH with DIC is safe.

2.2. Take an aliquot of 10 mM dimerizer from –80 °C and dilute in imaging medium to a stock concentration of 10 µM and store at –20 °C.

2.3. When ready to use, dilute dimerizers from 10 µM stock solution to a final working concentration of 100 nM in growth medium (for fixed imaging) or imaging medium. Treat cells with 100 nM dimerizers (final concentration) on stage for live imaging or incubate for 4–5 h for immunofluorescence (IF) and fluorescence in situ hybridization (FISH).

NOTE: The concentration of dimerizers used affects dimerization efficiency and thus phase

separation. The dimerizer concentration allowing maximum dimerization efficiency depends on cell type and anchor protein concentration, so it will need to be determined for different experiments. One simple way is to incubate cells expressing the anchor protein and mCherry-eDHFR (without fusing to the phase separating protein or fused to a non-phase separating mutant) and identify the dimerizer concentration at which the highest mCherry intensity at the anchor is achieved. A more systematic approach is to incubate cells expressing the anchor only with different concentrations of dimerizers and then with a Halo binding dye to help determine the dimerizer concentration at which the Halo binding dye intensity starts to plateau (i.e., all Halo-fused anchors are occupied by the dimerizer and no more left for the Halo binding dye)³².

2.4. To reverse dimerization, incubate cells with dimerizers for 2–5 h (with or without live imaging) or until desired droplet size is achieved and add 100 μ M free TMP (final concentration) diluted in imaging medium to cells.

3. Immunofluorescence (IF)

3.1. Seed 10^5 cells on 12 mm diameter circular cover glasses coated with poly-D-lysine in 6-well plate. Then transfect the two plasmids (Halo-GFP-TRF1 with mCherry-eDHFR-SIM or mCherry-eDHFR-SIM mutant) and wait for 24–48 h before proceeding to immunofluorescence.

NOTE: Wait more than one day after transfection can obtain higher expression.

3.2. Dilute dimerizers with growth medium to reach a final concentration of 100 nM, add diluted dimerizers to cells and incubate at 37 °C for 4–5 h.

NOTE: Phase separation is quickly induced after adding dimerizers (<30 min). Longer incubation helps droplets coarsen into larger sizes. Following droplet growth with live imaging can be used to determine the time it takes for droplets to reach a desired state.

3.3. Fix cells in PBS solution containing 4% formaldehyde and 0.1% Triton X-100 for 10 min at room temperature to permeabilize cells. Wash cells three times with PBS.

NOTE: After this step, pause the protocol and store the cells at 4 °C for up to a week.

CAUTION: Formaldehyde is harmful if inhaled or swallowed; it also irritates eyes, respiratory system, and skin and is a possible cancer hazard. Need to wear personal protective equipment, use only in a chemical fume hood. Also put it in a waste container after use, do not dispose it in the sink.

3.4. Wash coverslips two times with 50 μ L of TBS-Tx and once with 50 μ L of Antibody Dilution Buffer (AbDil). TBS-Tx was made by TBS, 0.1% Triton X-100 and 0.05% Na-azide. AbDil was made by TBS-Tx, 2% BSA, and 0.05% Na-azide.

3.5. Incubate each coverslip with 50 μ L of primary anti-PML (1:50 dilution in AbDil) / anti-

SUMO1 (1:200 dilution in AbDil) / anti-SUMO2/3 antibody (1:200 dilution in AbDil) at 4 °C in a humidified chamber overnight. mCherry antibody can also be used (1:200 dilution in AbDil) to help detect mCherry signal for FISH.

NOTE: FISH quenches the mCherry fluorescent signal, which makes it difficult to differentiate cells transfected with mCherry plasmids from those not transfected in FISH experiments. Using mCherry antibody is advised. Alternatively, one can make a stable cell line expressing eDHFR containing protein.

3.6. Wash coverslips three times with AbDil to remove unbound primary antibody.

3.7. Incubate cells with secondary antibody [anti-mouse IgG (H+L) secondary antibody conjugated with Alexa Fluor 647 for PML and SUMO, anti-rabbit IgG (H+L) secondary antibody conjugated with Alexa Fluor 555 for mCherry, both at 1:1000 dilution in AbDil] for 1 h in a dark box at room temperature.

3.8. Wash coverslips three times with TBS-Tx.

3.9. Label slides, dilute DAPI in mounting media to reach DAPI final concentration of 1 µg/mL. Then put 2 µL diluted DAPI on the slide. Flip the coverslips over and place them onto DAPI drop, aspire extra fluid from the edge of the coverslip.

3.10. Seal with nail polish, let it dry and rinse from the top of the coverslip with water. Save in the freezer for imaging.

4. Fluorescence in situ hybridization (FISH)

4.1. Seed 10^5 cells on 12 mm diameter circular cover glasses coated with poly-D-lysine in 6-well plate. Transfected cells with Halo-TRF1 and mCherry-eDHFR-SIM or mCherry-eDHFR-SIM mutant plasmids.

NOTE: Here, TRF1 is not fused with GFP to free the green channel up for the telomere DNA probe.

4.2. Fix cells with 4% formaldehyde for 10 min at room temperature and wash four times with PBS. For IF-FISH, after washing off secondary antibody in IF (3.8), refix cells with 4% formaldehyde for 10 min at room temperature and wash four times with PBS.

4.3. Dehydrate the coverslips in an ethanol series (70%, 80%, 90%, 2 min each).

4.4. Incubate the coverslips with 488-telC PNA probe (1:2000 ratio) in 5 µL of hybridization solution at 75 °C for 5 min. The hybridization solution contains 70% deionized formamide, 10 mM Tris (pH 7.4), and 0.5% blocking reagent. Then, incubate overnight in a humidified chamber at room temperature.

4.5. Wash the coverslips with wash buffer (70% formamide, 10 mM Tris) 2 min three times at room temperature and mount with 1 μ g/mL DAPI in mounting media for imaging.

NOTE: The FISH protocol is a published protocol^{33,34}.

5. Live imaging

5.1. When the cells are ready for imaging, mount the coverslips in magnetic chambers with cells maintained in 1 mL imaging medium without phenol red on a heated stage in an environmental chamber.

5.2. Set up microscope and environmental control apparatus. Images were acquired with a spinning disk confocal microscope with a 100x 1.4 NA objective, a Z-Drive, a camera, and a laser merge module equipped with 455, 488, 561, 594, and 647 nm lasers controlled by software. All lasers are 20 mW measured at the objective.

5.3. Locate cells with bright GFP signal on telomeres and diffusive mCherry signal in the cytosol. Find around 20 cells, memorize each position with x,y,z information and set up parameters for time lapse imaging with 0.5 μ m spacing for a total of 8 μ m in Z and a 5 min time interval for 2–4 h for both GFP and mCherry channels. Use 30% of 594 nm and 50% of 488 nm power intensity, with exposure times of 200 ms and camera gain 300.

NOTE: The output power of laser units is 20 mW. Bright GFP foci indicate larger anchor size, which can nucleate condensates more easily. Find cells with a wide range of mCherry signal because phase separation depends on SIM concentration in the cell. Cells with too dim or too bright mCherry signal may not phase separate. Do not to use too much laser power or too long exposure time to avoid photobleaching.

5.4. Start imaging and take one-time loop as pre-dimerization. Pause imaging, add 0.5 mL imaging media containing 15 μ L of 10 μ M dimerizer to the imaging chamber on the stage so that the final dimerizer concentration is 100 nM. Resume imaging.

5.5. When ready to reverse dimerization, pause imaging, add 0.5 mL of imaging media containing 2 μ L of 100 mM stock TMP to the imaging chamber on the stage to get 100 μ M TMP final concentration. Continue imaging cells for 1–2 h.

6. Fixed imaging

6.1. Use the same microscope set up as live imaging, stage heating is not needed. Use 488 nm to image telomere FISH, 561 nm for mCherry IF, and 647 nm for PML or SUMO IF.

NOTE: If not using a mCherry antibody, just directly image mCherry protein but signal maybe dim because of quenching in FISH. Still use 561 nm rather than 594 nm laser to image mCherry to avoid signal bleed-through of Cy5 to mCherry.

6.2. Locate around 30–50 cells with red signal (mCherry or mCherry IF) to select for transfected cells.

6.3. Take images with 0.3 μm spacing for a total of 8 μm in Z for collecting more signals. Use 80% of 647 nm, 80% of 561 nm, and 70% of 488 nm power intensity, with exposure times of 600 ms and camera gain 300.

7. Process time-lapse images

7.1. Define binary for telomeres

7.1.1. Choose one cell with all time and z-stack information, choose only GFP channel and create binary layer by defining the threshold. Adjust the lower and upper values of the threshold and use functions such as “Smooth”, “Clean”, and “Fill holes” to see how well the threshold picks up the desired objects through all time points.

7.2. Subtract background

7.2.1. Choose all channel, draw rectangle Region of Interest (ROI) on the background (aside from the cell). Define this ROI as background and then subtract background intensity.

7.3. Link telomere binary to telomere intensity

7.3.1. Choose telomere binary and link it to the GFP channel for calculating GFP intensity in the binary objects as telomere intensity.

7.4. Calculate telomere number and intensity over time

7.4.1. Specify which information to be exported, such as time, object ID, mean intensity, and sum intensity and export data to excel. Use MATLAB to read the excel and generate figures of telomere numbers and telomere intensity (summarize intensity over the volume in each telomere and then average over all telomeres in a cell) over time.

8. Process fixed-cell images

8.1. Define binary for APBs

8.1.1. Choose transfected cells for analysis by looking for signal in 561 nm channel. Following the procedure in step 7.1, define threshold in both GFP (telomere DNA FISH) and Cy5 (PML or SUMO IF) channel to generate binary for telomeres and PML bodies or SUMO, respectively. Merge GFP and Cy5 binary layers and create a new layer containing particles that have both GFP and Cy5 signals to represent co-localization of PML body on telomeres, thus APBs.

8.2. Calculate APB/SUMO number and intensity

8.2.1. Subtract image background following step 7.2. Link APB/SUMO binary layer to Cy5 channel following step 7.3. Calculate APB/SUMO number and intensity and export data to excel following step 7.4.

REPRESENTATIVE RESULTS:

Representative images of telomeric localization of SUMO identified by telomere DNA FISH and SUMO protein IF are shown in **Figure 2**. Cells with SIM recruitment enriched SUMO1 and SUMO 2/3 on telomeres compared to cells with SIM mutant recruitment. This indicates that SIM dimerization-induced SUMO enrichment on telomeres depends on SUMO-SIM interactions.

A representative time lapse movie of TRF1 and SIM after dimerization is shown in **Video 1**. Snapshots at four timepoints are shown in **Figure 3A**. SIM was successfully recruited to telomeres and both SIM and TRF1 foci became larger and brighter, as predicted for liquid droplet formation and growth (**Figure 1B**). In addition, fusion of TRF1 foci was observed (**Figure 3B**), which led to telomere clustering as shown in the reduced telomere number (**Figure 3E**) and increased telomere intensity over time (**Figure 3D**). In contrast, SIM mutant was recruited to telomeres after dimerization but did not induce any droplet formation or telomere clustering (**Figure 3C,D,E, Video 2**). This indicates that phase separation and thus telomere clustering is driven by SUMO-SIM interactions.

The reversal of phase separation and telomere clustering after adding excess free TMP is shown in **Video 3**. Snapshots at four timepoints are shown in **Figure 4A**. Agreeing with the predicted condensate dissolution and de-clustering of telomeres, telomere number increased, and telomere intensity decreased over time (**Figure 4B, C**).

Representative images of APBs identified by telomere DNA FISH and PML protein IF are shown in **Figure 5**. Cells with SIM recruited have more APBs than cells with SIM mutant recruited, suggesting dimerization-induced condensates are indeed APBs.

The figures here show representative images. For statistical analysis with more cells, please refer to Zhang et. al., 2020¹¹.

FIGURE AND TABLE LEGENDS:

Figure 1: Chemical dimerization to induce chromatin-associated condensates. (A) Dimerization schematic: The dimerizer consists of two linked ligands, TMP and Halo that interact with eDHFR and Haloenzyme, respectively. The phase separating protein is fused to mCherry and eDHFR, and the chromosome anchor protein is fused to Halo and GFP. (B) Before adding dimerizer (top-left nucleus), the majority of chromosome anchor proteins (green squares) are localized to the chromosomes and a small amount of anchor proteins are diffusely localized in the nucleoplasm. Phase separating proteins to be recruited (purple stars) and phase separating partners (proteins that will condense with the phase separating protein, red triangles) are diffusely localized in the

nucleoplasm. After adding dimerizers (top-right nucleus), phase separating proteins are dimerized to the anchor protein on the chromosomes and in the nucleoplasm. There could be some excess phase separating proteins in the nucleoplasm, depending on the relative concentration of the anchor protein, phase separating protein and the dimerizer used. After dimerization (bottom-right nucleus), local concentrating of the phase separating proteins at the anchor leads to phase separation and the formation of chromatin-associated condensates. Phase separating partners are enriched at the anchor because of co-condensation with the eDHFR-fused phase separating protein. Anchor proteins that are not directly bound to the chromatin can be enriched at the anchor because of dimerization to the phase separating protein. After adding excess free TMP to compete with the dimerizer for eDHFR binding (bottom-left nucleus), the phase separating protein is released from the chromatin and the condensate is dissolved.

Figure 2: SUMO is enriched after recruiting SIM to telomeres with dimerizers. (A) Dimerization schematic in this experiment: SIM (or SIM mutant) is fused to mCherry and eDHFR, and TRF1 is fused to Halo and GFP. (B) A representative cell for telomere DNA FISH and SUMO1 IF after recruiting SIM. Bottom is binary layer identifying telomeres, SUMO1 and number of colocalized SUMO1 and telomere DNA foci. Scale bars: 5 μ m. (C) A representative cell for telomere DNA FISH and SUMO1 IF after recruiting SIM mutant. At the bottom is the binary layer of the images used to identify the number of colocalized SUMO1 and telomere DNA foci. Scale bars: 5 μ m. (D) A representative cell for telomere DNA FISH and SUMO2/3 IF after recruiting SIM. At the bottom is the binary layer identifying telomeres, SUMO2/3, and the number of colocalized SUMO2/3 and telomere DNA foci. Scale bars: 5 μ m. (E) A representative cell for telomere DNA FISH and SUMO2/3 IF after recruiting SIM mutant. At the bottom is the binary layer of the images used to identify the number of colocalized SUMO2/3 and telomere DNA foci. Scale bars: 5 μ m.

Figure 3: Dimerization-induced phase separation drives telomere clustering. (A) Snapshots of TRF1-GFP and SIM-mCherry before and after adding 100 nM dimerizer (final concentration). At the bottom is the telomere binary layer identified from TRF1-GFP. Scale bars: 5 μ m. (B) A fusion event after recruiting SIM to telomeres. Scale bars: 2 μ m. Time interval: 5 min. (C) Snapshots of TRF1-GFP and SIM mutant-mCherry before and after adding 100 nM dimerizer (final concentration). At the bottom is the telomere binary layer identified from TRF1-GFP. Scale bars: 5 μ m. (D) Average telomere intensity (summarize intensity over the volume in each telomere and then average over all telomeres in a cell) over time after recruiting SIM (green, for cell in **Figure 3A**) and SIM mutant (blue, for cell in **Figure 3C**). (E) Telomere number over time after recruiting SIM (green, for cell in **Figure 3A**) and SIM mutant (blue, for cell in **Figure 3C**).

Figure 4: Reversal of condensation and telomere clustering. (A) Snapshots of TRF1-GFP and SIM-mCherry after adding 100 μ M TMP (final concentration) to cells with condensates formed for 3 h. At the bottom is the telomere binary layer identified from TRF1-GFP. Scale bars: 5 μ m. (B) Average telomere intensity (summarize intensity over the volume in each telomere and then average over all telomeres in a cell) over time for cell in **Figure 4A**. (C) Telomere number over time for cell in **Figure 4A**.

Figure 5: Dimerization-induced condensates are APBs. (A) A representative cell for telomere

DNA FISH and PML IF after recruiting SIM. At the bottom is the binary layer identifying telomeres, PML bodies and the number of colocalized PML and telomere DNA foci, i.e., number of APBs. Scale bars: 5 μ m. **(B)** A representative cell for telomere DNA FISH and PML IF after recruiting SIM mutant. At the bottom is the binary layer of the images used to identify the number of colocalized PML and telomere DNA foci, i.e., number of APBs. Scale bars: 5 μ m.

Video 1: Recruiting SIM with dimerizers to telomeres drives phase separation and telomere clustering. Live imaging of SIM-mCherry, TRF1-GFP, and merge channels before and after adding 100 nM dimerizer (final concentration). Scale bars: 5 μ m. Time interval: 5 min. Time as shown.

Video 2: Recruiting SIM mutant cannot drive phase separation and telomere clustering. Live imaging of SIM mutant-mCherry, TRF1-GFP and merge channels before and after adding 100 nM dimerizer (final concentration). Scale bars: 5 μ m. Time interval: 5 min. Time as shown.

Video 3: Reversal of condensation and telomere clustering. Live imaging of SIM-mCherry, TRF1-GFP and merge channels after adding 100 μ M TMP (final concentration) to cells with condensates formed for 3 h. Scale bars: 5 μ m. Time interval: 5 min. Time as shown.

DISCUSSION:

This protocol demonstrated the formation and dissolution of condensates on telomeres with a chemical dimerization system. Kinetics of phase separation and droplet-fusion-induced telomere clustering is monitored with live imaging. Condensate localization and composition are determined with DNA FISH and protein IF.

There are two critical steps in this protocol. The first is to determine protein and dimerizer concentration. The success in inducing local phase separation at a genomic locus relies on the increase in local concentration of the phase separating protein above the critical concentration for phase separation (**Figure 1B**). The global concentration of the phase separating protein needs to be high enough so that there are enough proteins to be concentrated locally. The concentration of the phase separating protein cannot be too high so that global phase separation has occurred or can be easily induced. The anchor DNA length (or size of the modified chromatin that the anchor protein binds to) and concentration of Halo-fused anchor protein determine the size of the nucleation center at maximum dimerization efficiency. The larger the anchor size the easy it is to nucleate condensates. The dimerization efficiency is affected by the amount of dimerizers relevant to the amount of anchor proteins. Too few dimerizers cannot occupy all the available anchor proteins while too many dimerizers result in non-productive binding of eDHFR to the excess dimerizers rather than to the ones on the anchor protein. Dimerizer concentration, along with the anchor DNA length and concentration of Halo-fused anchor protein, can be used to determine the critical concentration required for nucleating local phase separation. A systematic approach to vary those parameters (anchor DNA length, anchor protein concentration, phase separation protein concentration, and dimerizer concentration) can help map a multi-dimensional phase diagram. However, if the interest is not in mapping phase diagram but forming chromatin associated-condensates such as the ones demonstrated here, it is very easy to simply pick cells with bright Halo-GFP signal (larger anchor size) and cells with a wide range of brightness

for mCherry-eDHFR (various phase separating protein concentration) to image with the dimerizer concentration for maximum dimerization determined in Protocol 2.3. The second critical step is to avoid photobleaching in live imaging. Different from global phase separation where droplets (bright mCherry foci labeling the phase separating protein) will emerge after phase separation, local condensation at genomic locations cannot be easily spotted by judging the presence of mCherry foci. This is because recruitment of the protein alone, without phase separation, to genomic loci will result in formation of mCherry local foci. Phase separation occurs after recruitment, so mCherry foci continue to become bigger and brighter after initial recruitment. The phase-separation-induced enrichment can occur in GFP channel (the anchor protein) as well, due to the dimerization of the anchor protein to the phase separation protein. Therefore, change of physical properties (size and intensity) of the foci over time rather than the presence of foci should be used to judge phase separation. While it might be difficult to differentiate dimerization or phase separation-induced enrichment of mCherry (prey protein) foci, enrichment of GFP (anchor protein) foci only occurs if there is phase separation (**Figure 3D**). Therefore, enrichment of anchor protein can be used to easily judge phase separation. Photobleaching resulted from high laser power or long exposure time during imaging makes it more difficult to judge phase separation from live imaging and therefore should be avoided as much as possible by adjusting imaging conditions. Note that increase in foci intensity and size over time are characteristics of LLPS but cannot be used as the sole evidence for LLPS. In the case presented here, droplet fusion was used as evidence for the formation of liquid droplets, which may not occur for smaller number of anchors or less mobile anchors. Without droplet fusion, other methods such as diffusion of condensate components and sensitivity to small molecule perturbation can be used to further confirm condensate formation^{8, 9, 11}.

Though this chemical dimerization system renders temporal resolution required for monitoring phase separation in live cells, it lacks spatial resolution at the cellular and subcellular level. Thanks to the modular design of the dimerizers, it is possible to make light-sensitive dimerizers by attaching a photocage to TMP, making the linker photosensitive or both^{12, 32, 35}. By simply switching dimerizers within the same engineered cell background for different applications, high spatial and temporal control of the dimerization, reversal of dimerization, or both with light can be achieved. We envision with those light-sensitive dimerizers, it will be able to control phase separation with high spatial and temporal precision. Compared to the available optogenetic tools to control phase separation through light sensitive proteins^{36, 37}, a disadvantage of the chemical dimerization system is that it can only reverse phase separation once. However, this system can maintain sustained recruitment and thus phase separation without light, which makes it more suitable for long-term live imaging applications such as to follow droplet growth or cellular consequences of phase separation. Meanwhile, the ability to treat a population of cells without light makes it convenient for biochemical assays such as those needed to determine condensate composition or changes in genome organization.

This method can be easily adapted to induce condensates at other locations on the genome. One can simply identify a protein that binds to the genomic location of interest and fuse it to Halo to use it as an anchor (**Figure 1B**). Alternatively, one can combine this with CRISPR and fuse dCas9 to Halo and use guide RNAs to anchor Halo to the genomic loci of interest³⁸. In addition, one can

anchor Halo to an ectopic DNA array (e.g., LacO) integrated into the genome by fusing Halo to the targeting protein (e.g., LacI). One can then use a bottom-up approach to assess the ability of a protein to phase separate locally on chromatin, how its phase separation ability is affected by protein truncations, mutations, or post-translational modifications, or how the condensate affects local functions such as chromatin modification, replication, or transcription. To summarize, this chemical dimerization system can be used to induce a wide range of condensates on various chromatin locations and is particularly suitable for investigating how the material properties and chemical composition of chromatin-associated condensates contribute to chromatin functions by combining long-term live imaging with biochemical assays.

ACKNOWLEDGMENTS:

This work was supported by US National Institutes of Health (1K22CA23763201 to H.Z., GM118510 to D.M.C.) and Charles E. Kaufman foundation to H.Z. The authors would like to thank Jason Tones for proofreading the manuscript.

DISCLOSURES:

The authors have nothing to disclose.

REFERENCES:

1. Shin, Y., Brangwynne, C. P. Liquid phase condensation in cell physiology and disease. *Science*. **357** (6357) (2017).
2. Banani, S. F., Lee, H. O., Hyman, A. A., Rosen, M. K. Biomolecular condensates: organizers of cellular biochemistry. *Nature Reviews Molecular Cell Biology*. **18** (5), 285–298 (2017).
3. Sabari, B. R., Dall’Agnese, A., Young, R. A. Biomolecular condensates in the nucleus. *Trends in Biochemical Sciences*. 1–17 (2020).
4. Strom, A. R. et al. Phase separation drives heterochromatin domain formation. *Nature*. **547** (7662), 241–245 (2017).
5. Larson, A.G. et al. Liquid droplet formation by HP1 α suggests a role for phase separation in heterochromatin. *Nature*. **547** (7662), 236–240 (2017).
6. Boija, A. et al. Transcription factors activate genes through the phase-separation capacity of their activation domains. *Cell*. **175** (7), 1842–1855.e16 (2018).
7. Hur, W. et al. CDK-Regulated phase separation seeded by histone genes ensures precise growth and function of histone locus bodies. *Developmental Cell*. **54** (3), 379–394.e6 (2020).
8. McSwiggen, D. T., Mir, M., Darzacq, X., Tjian, R. Evaluating phase separation in live cells: diagnosis, caveats, and functional consequences. *Genes & Development*. **33** (23–24), 1619–1634 (2019).
9. Peng, A., Weber, S. C. Evidence for and against liquid-liquid phase separation in the nucleus. *Non-coding RNA*. **5** (4) (2019).
10. Erdel, F. et al. Mouse heterochromatin adopts digital compaction states without showing hallmarks of HP1-driven liquid-liquid phase separation. *Molecular Cell*. **78** (2), 236–249.e7 (2020).
11. Zhang, H. et al. Nuclear body phase separation drives telomere clustering in ALT cancer cells. *Molecular Biology of the Cell*. **31** (18), 2048–2056 (2020).
12. Ballister, E. R., Aonbangkhen, C., Mayo, A. M., Lampson, M. A., Chenoweth, D. M. Localized light-induced protein dimerization in living cells using a photocaged dimerizer. *Nature*

573 *Communications*. **5**, 1–9 (2014).

574 13. Yeager, T. R. et al. Telomerase-negative immortalized human cells contain a novel type of
575 promyelocytic leukemia (PML) body. *Cancer Research*. **59** (17), 4175–4179 (1999).

576 14. Zhang, J. M., Zou, L. Alternative lengthening of telomeres: From molecular mechanisms
577 to therapeutic outlooks. *Cell and Bioscience*. **10** (1), 1–9 (2020).

578 15. Corpet, A. et al. PML nuclear bodies and chromatin dynamics: catch me if you can! *Nucleic*
579 *Acids Research*. 1–23 (2020).

580 16. Li, Y., Ma, X., Wu, W., Chen, Z., Meng, G. PML nuclear body biogenesis, carcinogenesis,
581 and targeted therapy. *Trends in Cancer*. **6** (10), 889–906 (2020).

582 17. Dilley, R. L., Greenberg, R. A. ALTERNative telomere maintenance and cancer. *Trends in*
583 *Cancer*. **1** (2), 145–156 (2015).

584 18. Sobinoff, A. P., Pickett, H. A. Alternative lengthening of telomeres: DNA repair pathways
585 converge. *Trends in Genetics*. **33** (12), 921–932 (2017).

586 19. Draskovic, I. et al. Probing PML body function in ALT cells reveals spatiotemporal
587 requirements for telomere recombination. *Proceedings of the National Academy of Sciences*. **106**
588 (37), 15726 LP–15731 (2009).

589 20. Zhang, J. M., Yadav, T., Ouyang, J., Lan, L., Zou, L. Alternative lengthening of telomeres
590 through two distinct break-induced replication pathways. *Cell Reports*. **26** (4), 955–968.e3 (2019).

591 21. Loe, T.K. et al. Telomere length heterogeneity in ALT cells is maintained by PML-
592 dependent localization of the BTR complex to telomeres. *Genes and Development*. **34** (9–10),
593 650–662 (2020).

594 22. Potts, P. R., Yu, H. The SMC5/6 complex maintains telomere length in ALT cancer cells
595 through SUMOylation of telomere-binding proteins. *Nature Structural and Molecular Biology*. **14**
596 (7), 581–590 (2007).

597 23. Chung, I., Leonhardt, H., Rippe, K. De novo assembly of a PML nuclear subcompartment
598 occurs through multiple pathways and induces telomere elongation. *Journal of Cell Science*. **124**
599 (21), 3603–3618 (2011).

600 24. Shen, T. H., Lin, H. K., Scaglioni, P. P., Yung, T. M., Pandolfi, P. P. The mechanisms of PML-
601 nuclear body formation. *Molecular Cell*. **24** (3), 331–339 (2006).

602 25. Shima, H. et al. Activation of the SUMO modification system is required for the
603 accumulation of RAD51 at sites of DNA damage. *Journal of Cell Science*. **126** (22), 5284–5292
604 (2013).

605 26. Yalçın, Z., Selenz, C., Jacobs, J. J. L. Ubiquitination and SUMOylation in telomere
606 maintenance and dysfunction. *Frontiers in Genetics*. **8** (MAY), 1–15 (2017).

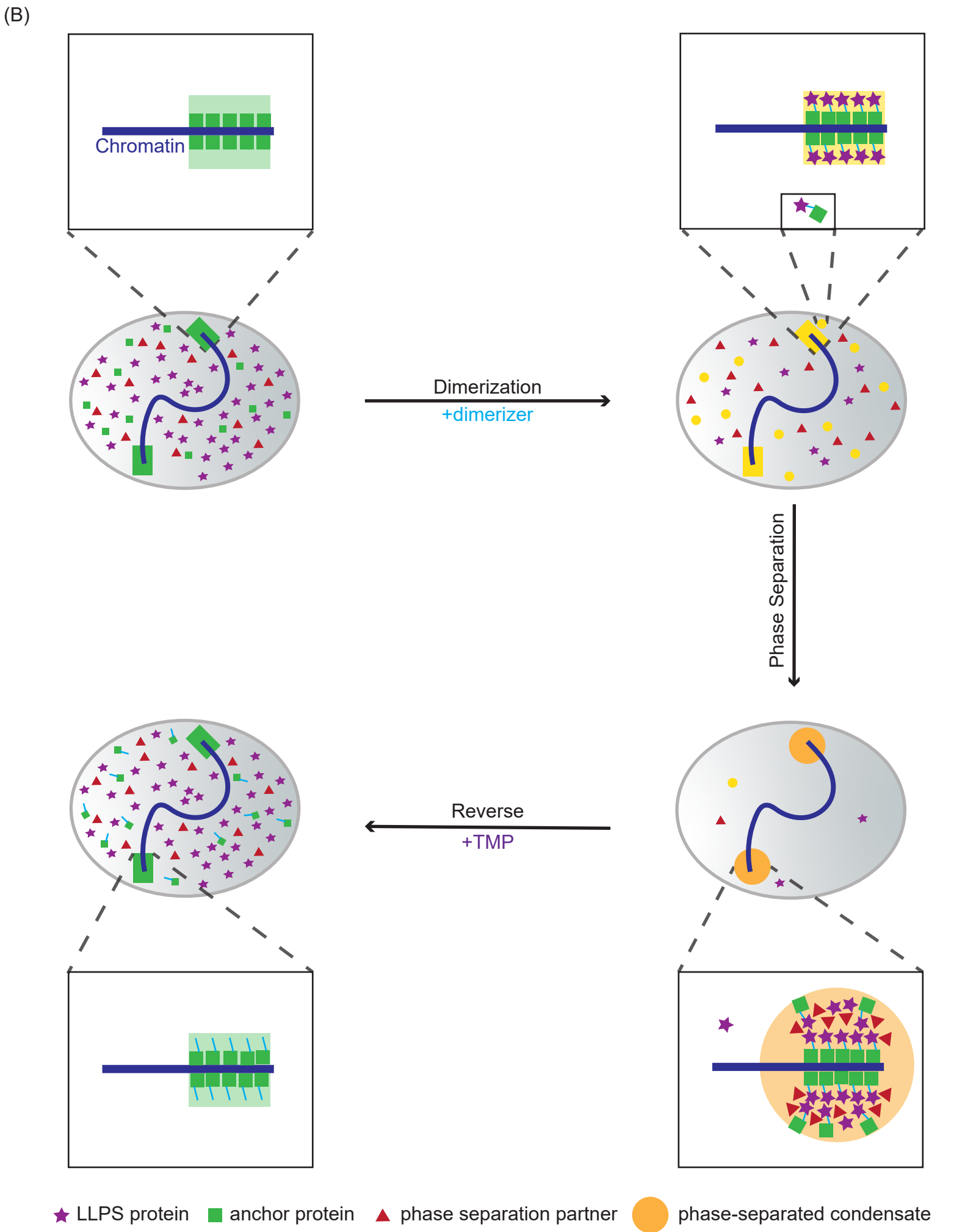
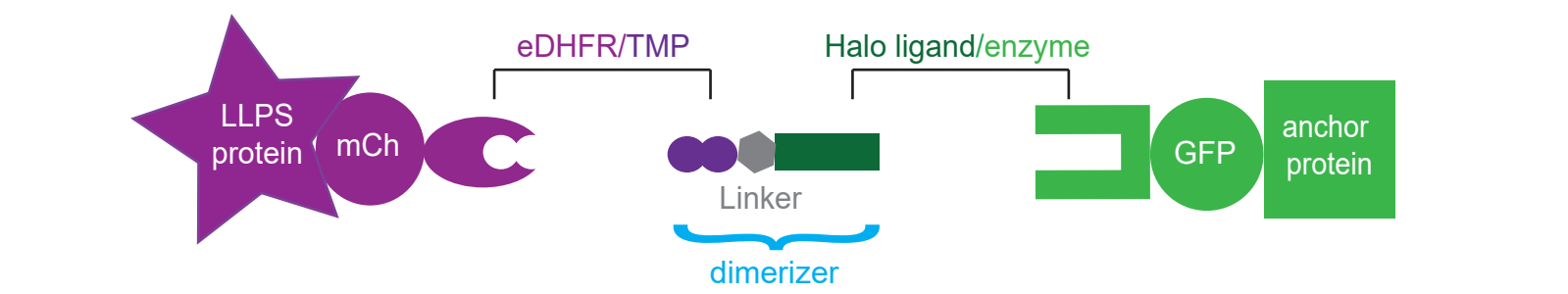
607 27. Sarangi, P., Zhao, X. SUMO-mediated regulation of DNA damage repair and responses.
608 *Trends in Biochemical Sciences*. **40** (4), 233–242 (2015).

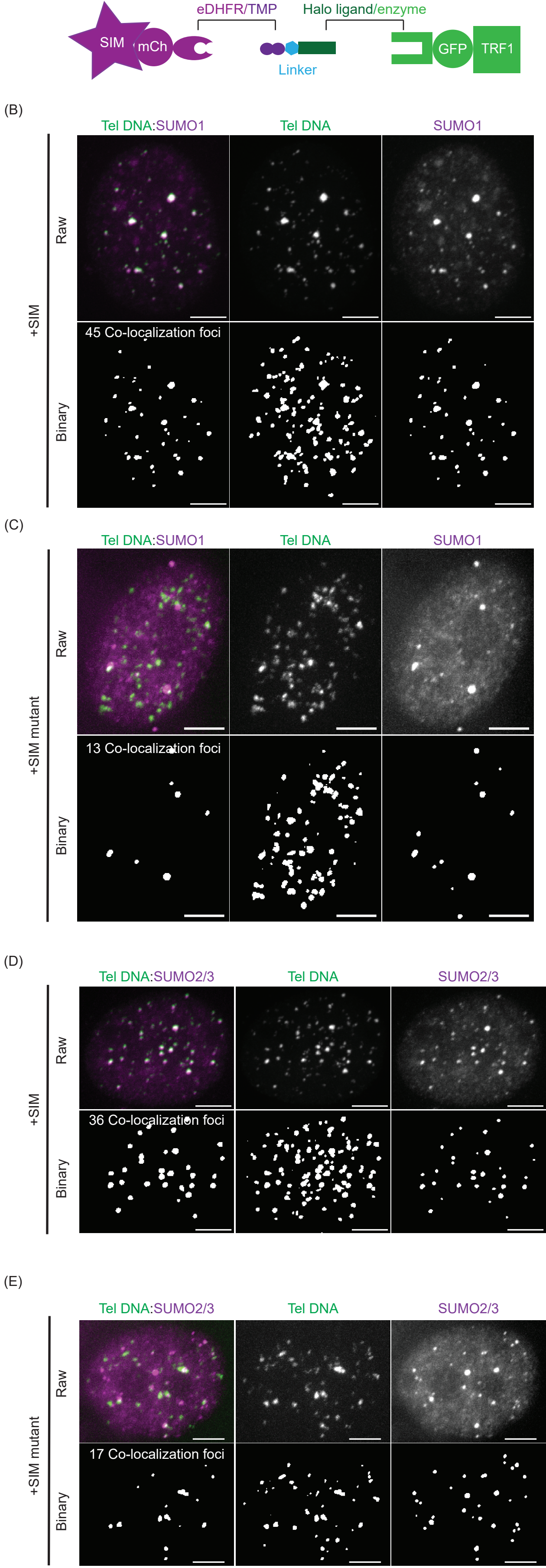
609 28. Banani, S. F. et al. Compositional control of phase-separated cellular bodies. *Cell*. **166** (3),
610 651–663 (2016).

611 29. Min, J., Wright, W. E., Shay, J. W. Clustered telomeres in phase-separated nuclear
612 condensates engage mitotic DNA synthesis through BLM and RAD52. *Genes and Development*.
613 **33** (13–14), 814–827 (2019).

614 30. Song, J., Durrin, L. K., Wilkinson, T. A., Krontiris, T. G., Chen, Y. Identification of a SUMO-
615 binding motif that recognizes SUMO-modified proteins. *Proceedings of the National Academy of*
616 *Sciences of the United States of America*. **101** (40), 14373–14378 (2004).

31. Zhang, H., Chenoweth, D. M., Lampson, M. A. Chapter 7 - Optogenetic control of mitosis with photocaged chemical dimerizers. *Mitosis and Meiosis Part A*. **144**, 157–164 (2018).
32. Zhang, H. et al. Optogenetic control of kinetochore function. *Nature Chemical Biology*. **13** (10), 1096–1101 (2017).
33. Cho, N. W., Dilley, R. L., Lampson, M. A., Greenberg, R. A. Interchromosomal homology searches drive directional ALT telomere movement and synapsis. *Cell*. **159** (1), 108–121 (2014).
34. Dilley, R.L. et al. Break-induced telomere synthesis underlies alternative telomere maintenance. *Nature*. **539** (7627), 54–58 (2016).
35. Aonbangkhen, C., Zhang, H., Wu, D. Z., Lampson, M. A., Chenoweth, D. M. Reversible control of protein localization in living cells using a photocaged-photocleavable chemical dimerizer. *Journal of the American Chemical Society*. **140** (38), 11926–11930 (2018).
36. Shin, Y. et al. Spatiotemporal control of intracellular phase transitions using light-activated optoDroplets. *Cell*. **168** (1–2), 159–171.e14 (2017).
37. Shin, Y. et al. Liquid nuclear condensates mechanically sense and restructure the genome. *Cell*. **175** (6), 1481–1491.e13 (2018).
38. Xiang, X. et al. CRISPR/Cas9-mediated gene tagging: a step-by-step protocol. *Methods in Molecular Biology*. **1961**, 255–269 (2019).





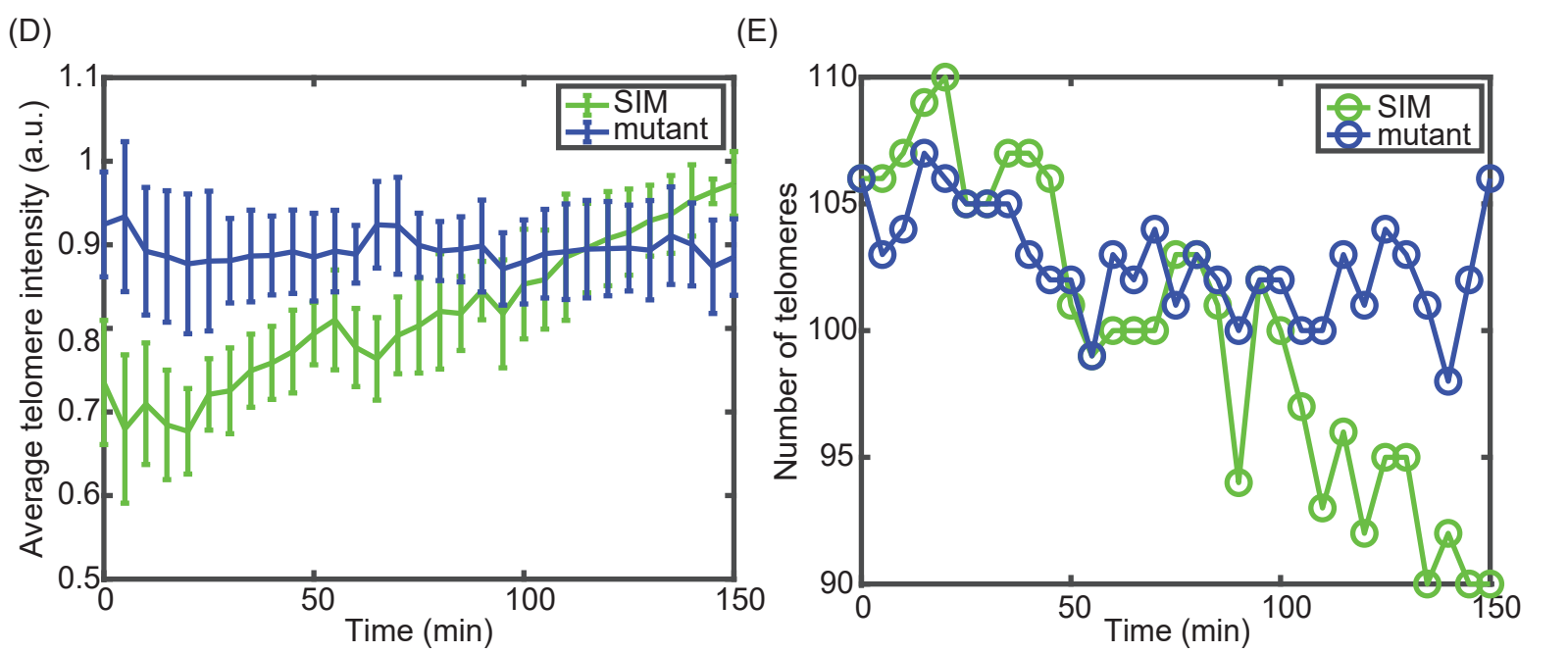
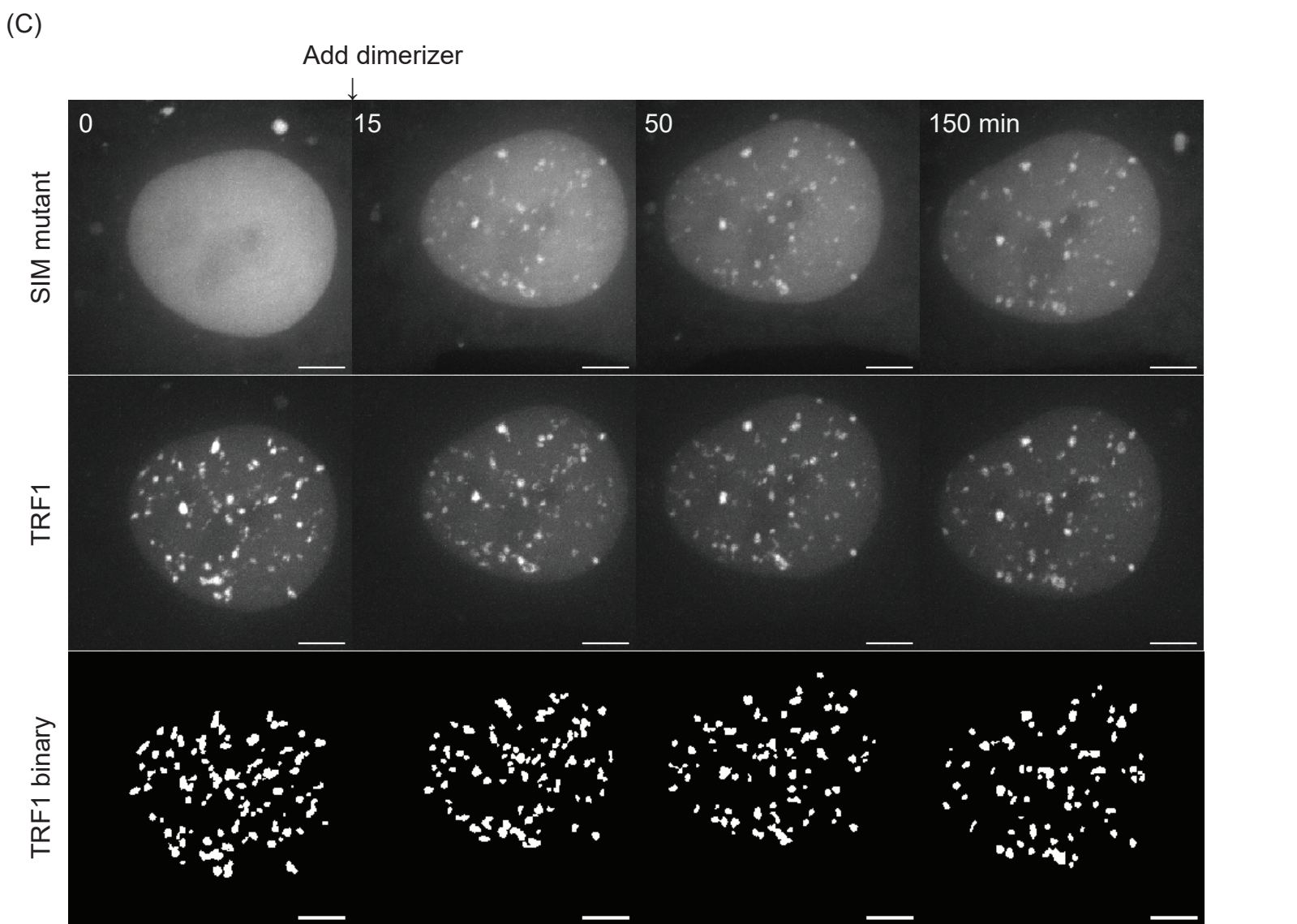
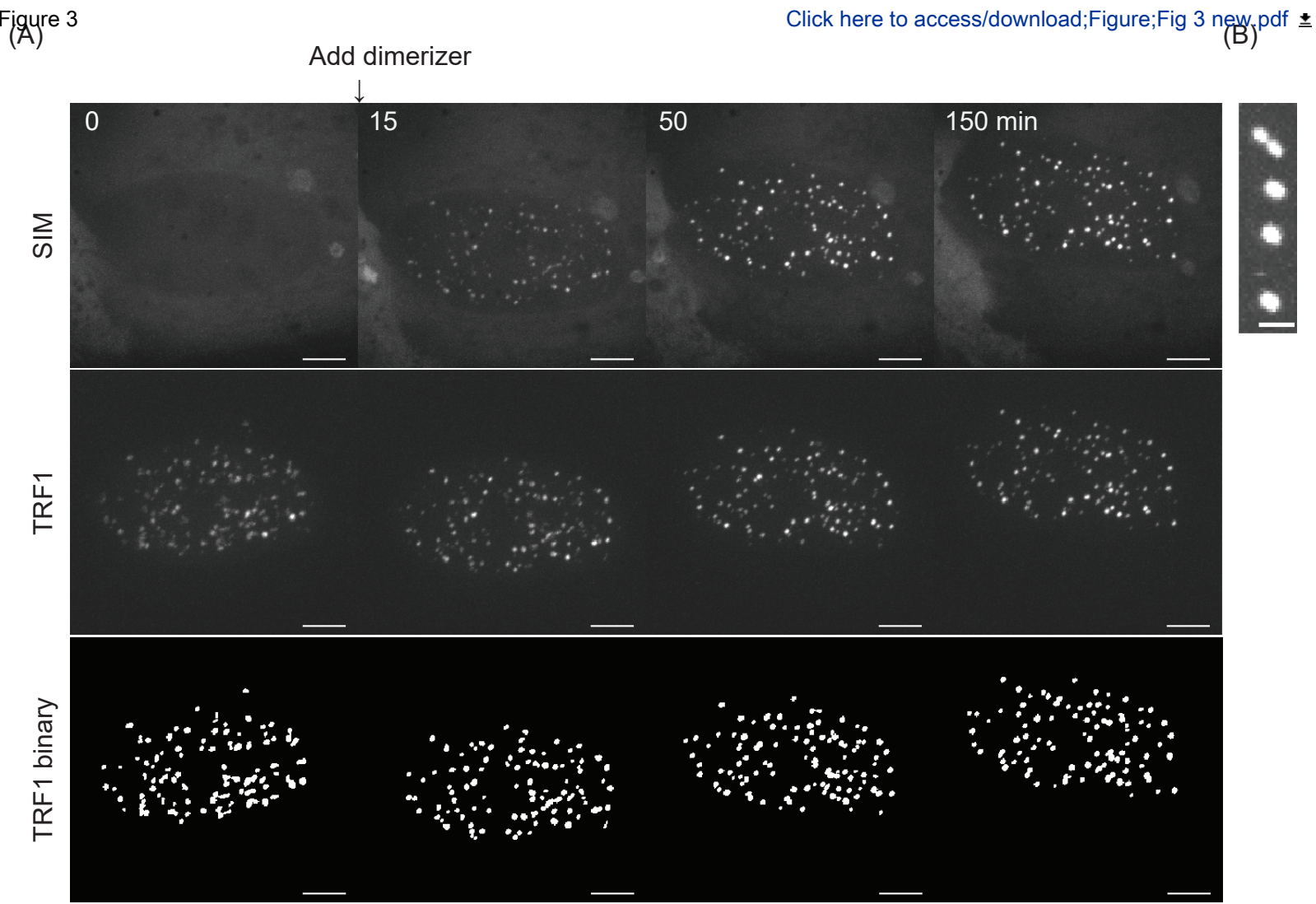
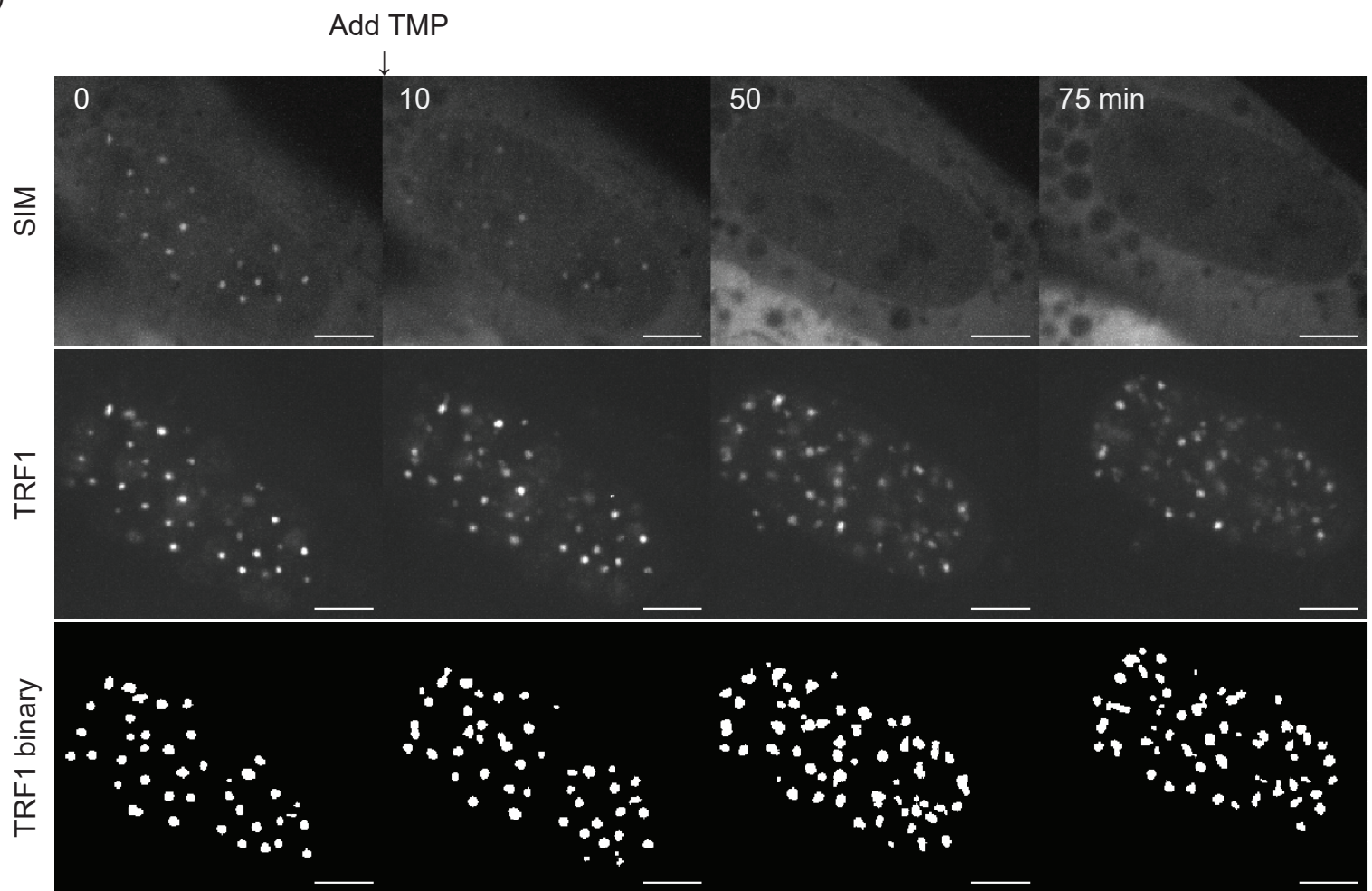
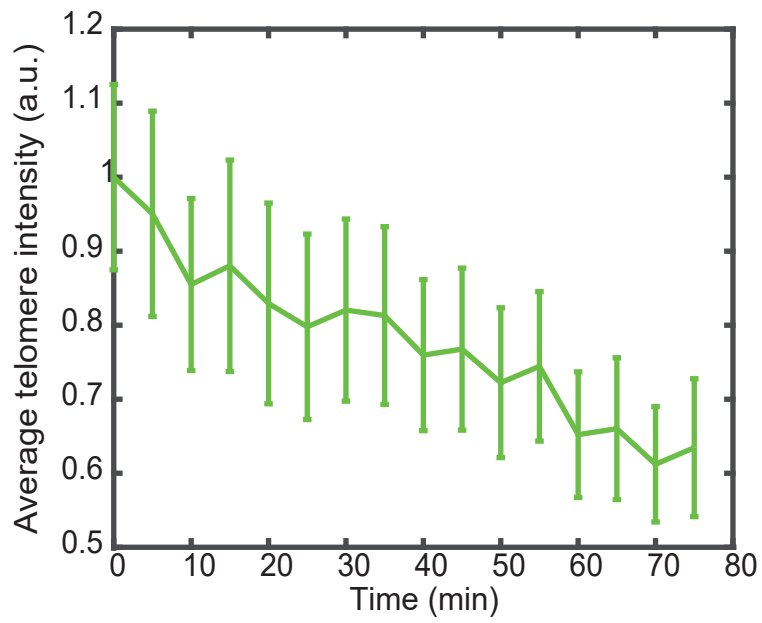


Figure 4
(A)

[Click here to access/download;Figure;Fig 4 new.pdf](#)



(B)



(C)

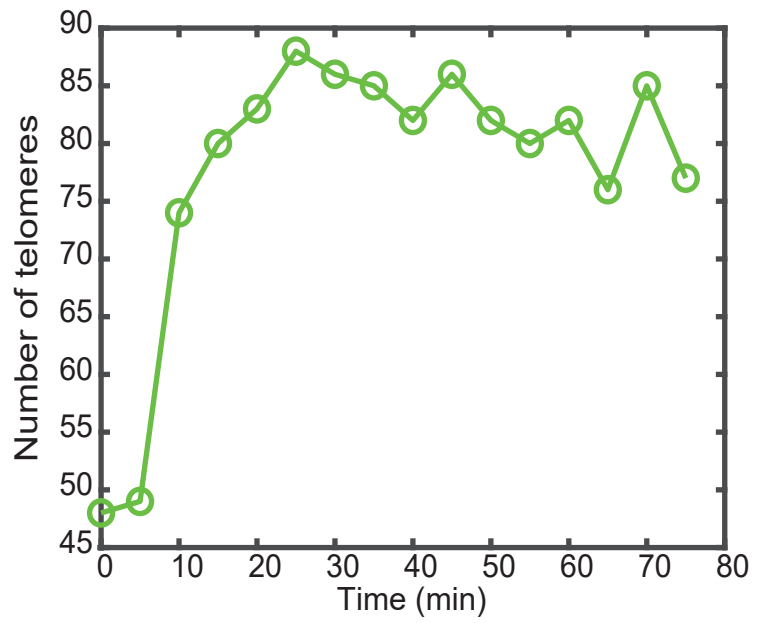
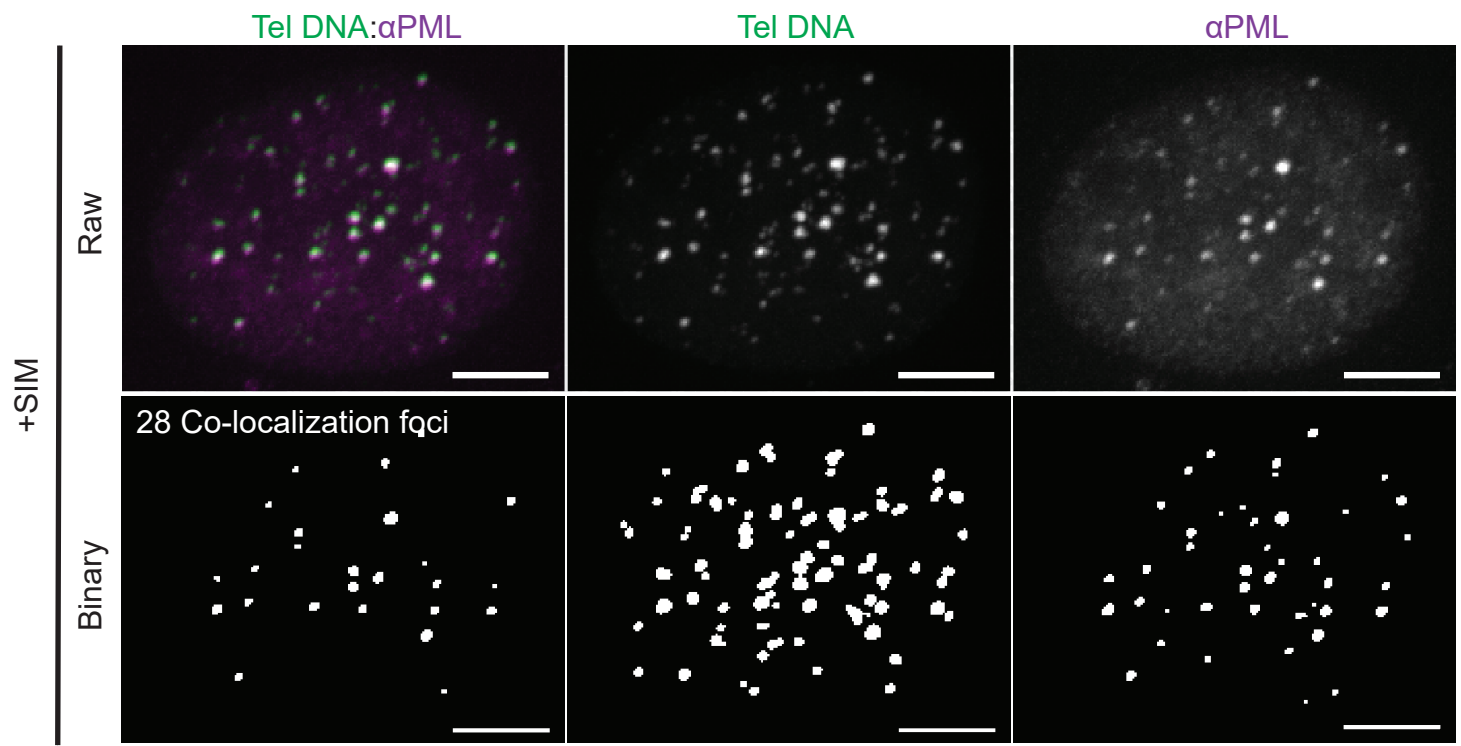
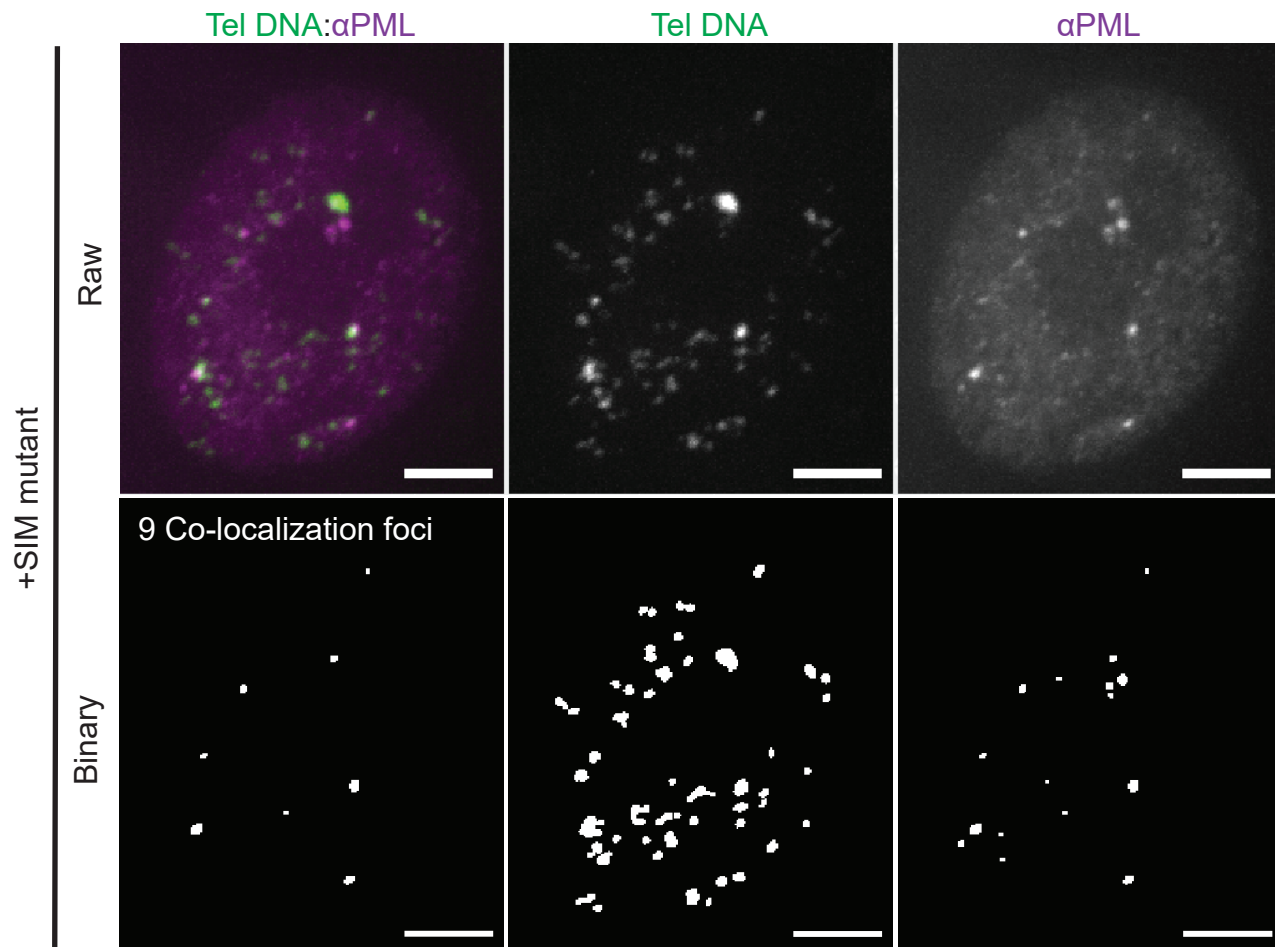


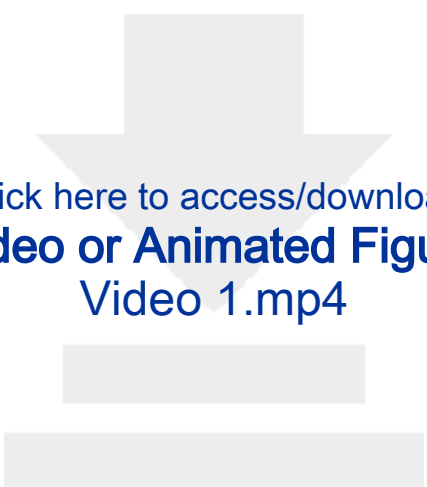
Figure 5
(A)

[Click here to access/download;Figure;Fig 5 new.pdf](#)

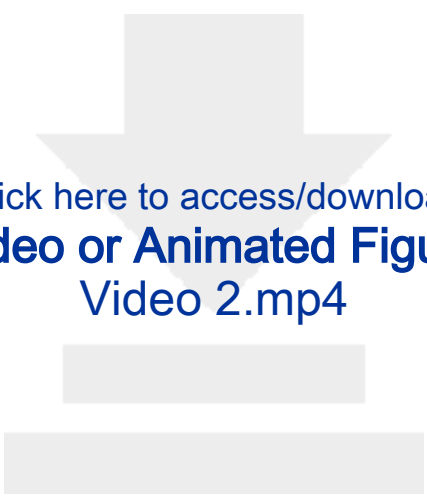


(B)

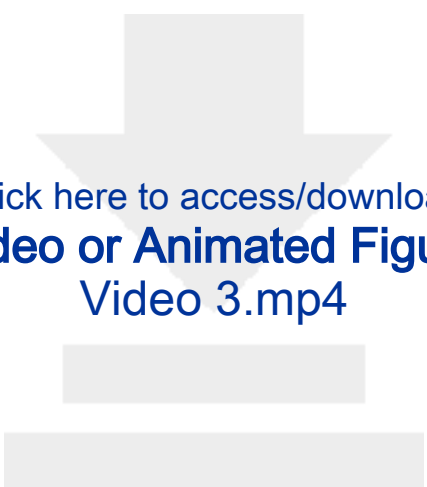




Click here to access/download
Video or Animated Figure
Video 1.mp4



Click here to access/download
Video or Animated Figure
Video 2.mp4



Click here to access/download
Video or Animated Figure
Video 3.mp4

Name of Material/ Equipment	Company	Catalog Number	Comments/Description
0.25% Trypsin, 0.1% EDTA in HBSS w/o Calcium, Magnesium and 16% Formaldehyde (w/v), Methanol-free	Corning	MT25053CI	Prepare 1% in 1x PBS
6 Well Culture Plate	Thermo Scientific	28906	
Aluminum Foil	VWR	10861-554	
Anti-mCherry antibody	Fisher Scientific	01-213-101	
Anti-PML antibody	Abcam	Ab183628	
Anti-SUMO1 antibody	Santa Cruz	sc966	
Anti-SUMO2/3 antibody	Abcam	Ab32058	
Blocking Reagent	Cytoskeleton	Asm23	
Bovine Serum Albumin (BSA)	Roche	11096176001	
BTX Tube micro 1.5ML	Fisher Scientific	BP9706100	
Circle Cover Slips	VWR	89511-258	
Confocal microscope	Thermo Scientific	3350	
DAPI	Nikon	MQS31000	
Dimethyl Sulphoxide	Fisher Scientific	D1306	
	Sigma-Aldrich	472301	
DMEM with L-Glutamine, 4.5g/L Glucose and Sodium Pyruvate	Corning	MT10017CV	
EMCCD Camera	iXon Life	897	
Ethanol	Fisher Scientific	4355221	
Fetal Bovine Serum, Qualified, USDA-approved Regions	Gibco	A4766801	
Formamide, Deionized	MilliporeSigma	46-101-00ML	
Goat anti-Mouse IgG (H+L), Recombinant Secondary Antibody, Alexa Fluor 647	Invitrogen	A28181	
Goat anti-Rabbit IgG (H+L), Recombinant Secondary Antibody, Alexa Fluor 647	Invitrogen	A32733	

High Precision Straight Tapered Ultra Fine Point Tweezers/Forceps	Fisher Scientific	12-000-122	
Laser merge module	Nikon	NIIMHF47180	
Leibovitz's L-15 Medium	Gibco	21083027	
Lipofectamine 2000 Transfection Reagent	Invitrogen	11668027	
Matlab	The MathWorks		
Microscope Slide Box	Fisher Scientific	34487	
Nail Polish	Fisher Scientific	50-949-071	
NIS-Elements	Nikon		
Opti-MEM Reduced Serum Media	Gibco	51985091	
Parafilm	Bemis	13-374-12	
PBS 10x, pH 7.4	Fisher Scientific	70-011-044	
Penicillin-Streptomycin Sollution,100X	Gibco	15140122	
Piezo Z-Drive	PI	91985	
Pipet Tips	VWR	10017	
Plain and Frosted Clipped Corner Microscope Slides	Fisher Scientific	22-037-246	
Poly-D-Lysine solution	Sigma-Aldrich	A-003-E	
Sodium Azide	Fisher Scientific	BP922I-500	
Spinning disk	Yokogawa	CSU-X1	
Square Cover Slips	Thermo Scientific	3305	
TBS 10x solution	Fisher Scientific	BP2471500	
TelC-Alexa488	PNA Bio	F1004	
TMP	Synthesized by Chenoweth lab		
TNH	Synthesized by Chenoweth lab		
Tris Solution	Fisher Scientific	92-901-00ML	
Triton X-100 10% Solution	MilliporeSigma	64-846-350ML	Prepare 0.5% in 1x PBS

U2Os cell line	ATCC	HTB-96
VECTASHIELD Antifade Mounting Medium	Vector Laboratories	NC9524612

Response to Editorial and Reviewer Comments.

Editorial comments:

Changes to be made by the Author(s):

1. Please take this opportunity to thoroughly proofread the manuscript to ensure that there are no spelling or grammar issues. Please define all abbreviations at first use (TNH, AbDil etc).

[We proofread the manuscript and we defined the abbreviations. We also asked Jason Tones whose first language is English to help find grammar issues.](#)

2. JoVE cannot publish manuscripts containing commercial language. This includes trademark symbols (TM), registered symbols ([®]), and company names before an instrument or reagent. Please remove all commercial language from your manuscript and use generic terms instead. All commercial products should be sufficiently referenced in the Table of Materials and Reagents.

For example: Optimem, lipofectamine, NIS-Elements software etc

[We removed commercial language from the manuscript.](#)

3. Please revise the text, especially in the protocol, to avoid the use of any personal pronouns (e.g., "we", "you", "our" etc.).

[We changed the text to avoid personal pronouns.](#)

4. Please highlight only up to 3 pages of the Protocol (including headings and spacing) that identifies the essential steps of the protocol for the video, i.e., the steps that should be visualized to tell the most cohesive story of the Protocol. Remember that non-highlighted Protocol steps will remain in the manuscript, and therefore will still be available to the reader.

[We un-highlighted Note section in the protocol to reduce it to 3 pages.](#)

5. Please include legends (title and description) for the three video files in the figure and table legends section.

[The legends for the three video files are added in the manuscript.](#)

6. Please sort the Materials Table alphabetically by the name of the material.

[We sorted the Materials Table alphabetically.](#)

Reviewers' comments:

Reviewer #1:

Manuscript Summary:

The last few years have witnessed the emergence of a novel paradigm to explain the compartmentalization of proteins within cells. The well described physical mechanism of liquid-liquid phase separation (LLPS) can indeed be applied in the context of cell biology and offers a new prism to consider how molecules may self-organize within cells. Upon specific biophysical conditions, biological macromolecules concentrate in a spontaneous manner in phase-separated liquid-like droplets that have been called biomolecular condensates. This phenomenon has brought a renewed interest in the mechanisms that shape and drive cellular responses to environmental stimuli. In this manuscript, the authors describe a novel method to induce protein condensates on a specific genomic locus, the telomeres, via a chemical dimerization system. This method, which has already been published by the authors in Zhang et al. Mol. Biol. of the Cell 2020, have proven effective to establish that APB coalescence can drive telomere clustering. While the manuscript will be undoubtedly be useful for scientists to establish the chemical dimerization system in their labs, it currently lacks accuracy in experiment details as well as a critical comparison with another type of system that allows to achieve the same goal (published in Min et al. G&D 2019, <http://www.genesdev.org/cgi/doi/10.1101/gad.324905.119>). This should be addressed before publication in JoVE.

Major Concerns:

- In the introduction section, the description of the relationship between LLPS and cell biology could be a bit more balanced. While it is now widely recognized that LLPS does play an important role in organizing cellular compartments and biochemical reactions, it is also highly debated whether "true" LLPS mechanisms apply in the case of transcription or heterochromatin formation (see for review A and Weber, 2019, doi:10.3390/ncrna5040050 or McSwiggen et al., 2019, <http://www.genesdev.org/cgi/doi/10.1101/gad.331520.119>). For example, the authors describe the LLPS properties of HP1 protein that is involved in the formation of heterochromatin domains (refs 4 and 5 in the manuscript : Larson et al., 2018 and Strom et al., 2018). While these papers have indeed made a landmark contribution by showing the LLPS properties of HP1, heterochromatin foci in vivo seem to lack liquid-like properties and may rather behave as collapsed polymer globules (see Erdel et al., Mol Cell 2020, <https://doi.org/10.1016/j.molcel.2020.02.005>, as well as Erdel and Rippe, 2018, <https://doi.org/10.1016/j.bpj.2018.03.011>).

We thank the reviewer for this insightful comment. We changed the introduction to the following so it is more balanced: However, despite many examples of chromatin-associated condensates being discovered, the underlying mechanisms of condensate formation, regulation and function remain poorly understood. In particular, not all chromatin-associated condensates are formed through LLPS and careful evaluations of condensate formation in live cells are still needed ^{8,9}. For example, HP1 protein in mouse is shown to have only a weak capacity to form liquid droplets in live cells and heterochromatin foci behave as collapsed polymer globules¹⁰.

- Concerning the introduction part on PML and ALT, references 11 and 12 are a bit out of date. Two recent reviews should be added: Corpet et al., NAR 2020 (doi:

10.1093/nar/gkaa828) and Li et al., Trends in Cancer 2020 (<https://doi.org/10.1016/j.trecan.2020.05.005>). In particular, they discuss the possible involvement of LLPS in PML NBs formation, an aspect that should be discussed more extensively in the introduction part. While it is well-proven that polySUMO-polySIM polymers undergo LLPS, phase transition properties of the PML protein itself have yet to be demonstrated. Thus, caution should be taken when stating "enrichment of... PML protein induces local phase separation to form APBs". It is the SUMO-SIM interactions that drive LLPS and in fact, the authors indeed use a SIM motif only (and not the PML protein) to induce protein condensation at telomeres. Here, addition of a figure showing SUMO recruitment to condensates could help to understand the LLPS formation via SIM-SUMO interactions at telomeres. PML, as a SUMO-SIM containing protein, is recruited in the condensate.

We thank the reviewer for this comment. We added the suggested references in Introduction. We added a new figure (Figure 2) to show that recruiting SIM on telomeres enriches SUMO1/2/3 to drive phase separation. We also changed Introduction to the following to reflect more clearly that it is SUMO-SIM interactions that drive phase separation: Since telomere proteins in ALT cells are uniquely modified by small ubiquitin-like modifier (SUMO)²², many APB components contain sumoylation sites^{22–25} and/or SUMO-interacting motifs (SIMs)^{26, 27} and SUMO-SIM interactions drive phase separation²⁸, we hypothesized that sumoylation on telomeres leads to enrichment of SUMO/SIM containing proteins and SUMO-SIM interactions between those proteins lead to phase separation. PML protein, which has three sumoylation sites and one SIM site, can be recruited to form APBs and coalescence of liquid APBs leads to telomeres clustering. To test this hypothesis, we used the chemical dimerization system to mimic sumoylation-induced APB formation by recruiting SIM to telomeres (Figure 2A)¹¹. GFP is fused to Haloenzyme for visualization and to the telomere-binding protein TRF1 to anchor the dimerizer to telomeres. SIM is fused to eDHFR and mCherry. Kinetics of condensate formation and droplet fusion-induced telomere clustering is followed with live cell imaging. Phase separation is reversed by adding excess free TMP to compete with eDHFR binding. Immunofluorescence (IF) and fluorescence in situ hybridization (FISH) is used to determine condensate composition and telomeric association. Recruiting SIM enriches SUMO on telomeres and the induced condensates contain PML and therefore are APBs. Recruiting a SIM mutant that cannot interact with SUMO does not enrich SUMO on telomeres or induce phase separation, indicating that the fundamental driving force for APB condensation is SUMO-SIM interaction.

- Regarding the ALT process, one recent review to be added could be the following : Zhang and Zou, 2020, <https://doi.org/10.1186/s13578-020-00391-6>). In addition, there is no mention nor discussion of the following paper : Min et al. G&D 2020, <http://www.genesdev.org/cgi/doi/10.1101/gad.324905.119>. This paper describes the use of another system to induce protein condensates at telomeres and follow their clustering. The authors have used the polySUMO-polySIM polymers, initially described in Banani et al., 2016, fused to the C-terminal domain of RAP1 that binds strongly to TRF2, with addition of NLS sequences. A critical discussion about the

similarities/disparities, advantages/disadvantages of such a system compared to the one described the authors should be of interest in such a method paper.

We thank the reviewer for this comment. We added the suggested review by Zhang et. al. and added the comparison of our system to that used by Min et.al. in the Introduction : Agreeing with this observation, APB formation can be induced with polySUMO-polySIM polymers that fused to a TRF2 binding factor RAP1³⁴. Compared to the polySUMO-polySIM fusion system where phase separation occurs as long as enough proteins are produced, the chemical dimerization approach presented here induces phase separation on demand and thus offers better temporal resolution to observe the kinetics of phase separation and telomere clustering process. In addition, this chemical dimerization system permits the recruitment of other proteins to assess their ability in inducing phase separation and telomere clustering. For example, a disordered protein recruited to telomeres can also form droplets and cluster telomeres without inducing APB formation, suggesting telomere clustering is independent of APB chemistry and only relies on APB liquid property¹¹.

- Experimental details are not accurate enough in order for an external reader to fully replicate the experiments.
- For example, on step 3.3, it is stated that cells are permeabilized in 0.5% Triton X-100: what is this reagent dissolved in ? PBS ? or TBS ? are there washing steps following fixation in 4% formaldehyde and prior to permeabilization?

The reagent is dissolved in PBS and permeabilization is in the same step with fixation. Yes, there is a wash step that was left out. We changed step 3.3 to : Fix cells in PBS solution containing 4% formaldehyde and 0.1% Triton X-100. Wash cells three times with PBS.

- Step 3.4 is not clear as well : "once with AbDil (add 50uL buffer to rinse)". It is not clear which buffer is added to rinse ? AbDil or TBS-Tx ? is 50uL enough to rinse a 12mm coverslip ?

We thank the reviewer for this comment. 50uL is enough to rinse a 12mm coverslip. To make it clearer, we changed to: Wash coverslips two times with 50 μ L TBS-Tx and once with 50 μ L Antibody Dilution Buffer.

- Step 3.9 : what is the amount of mounting medium ? this is important to know the final DAPI concentration (addition of 2uL of DAPI at 1ug/mL does not mean anything if we don't know the dilution ratio).

The mounting media is 2uL. We changed the text to make it clear: Dilute DAPI in mounting media to reach DAPI final concentration of 1 μ g/mL. Then put 2 μ L diluted DAPI on the slide.

- The FISH protocol is not very standard and this could be explained. For example,

incubation of the probe is performed at room temperature versus 37°C in most cases. Washes are usually performed with SSC solutions of various concentrations at various temperatures. Here, there is no mention of the temperature used for FISH washes, which can be highly critical.

We washed at room temperature; this information is now added. We follow published protocol from Cho et al., 2014, doi: 10.1016/j.cell.2014.08.030 and Dilley et al., 2016, doi:10.1038/nature20099 used for telomere FISH. We've added the references as ref 32 and 33 to the manuscript.

- Concerning the plasmid constructions, more details should be provided. Are they available ? what is the SIM sequence used ? from which protein ? how many SIMs are present ?

We thank the reviewer for this comment. We are depositing plasmids Halo-GFP-TRF1, mCherry-eDHFR-SIM, mCherry-eDHFR-SIM mutant to addgene. We also added the sequence information for SIM: SIM is from PIASx²⁸. SIM sequence is AAAGTCGATGTAATTGACTTAACGATCGAATCTAGCAGCGATGAAGAAGAAGATCCACCGGCTAAACGT. SIM mutant is generated by mutating SIM amino acid VIDL to VADA²⁸, and the sequence is AAAGTCGATGTAGCCGACGCCACGATCGAATCTAGCAGCGATGAAGAAGAAGATCACCGGCTAAACGT.

Minor Concerns:

- in Figure 1 : it is not clear whether addition of TMP only disrupts binding of LLPS-mCherry-eDHFR protein to the linker, or if the linker also detaches from the Halo enzyme. If not, in the zoom of the top left nucleus, the linker should still be attached to the anchor protein (but without any LLPS protein bound to it).

Yes, linker shouldn't be detached from Halo and we added another step in figure 1 to reflect this.

- in Figure 3B the number of telomeres does not match to images presented in figure 3A. 40 to 58 (approximately) telomeres foci (counted in the TRF1 binary image) are presented in figure 3A. How do the authors explain the discrepancy with the numbers presented on the graph (75 to 100 telomeres) ?

We thank the reviewer pointing this discrepancy out. We plotted data from a different cell by mistake and we've changed the two plots to match the cell in Figure 4A. We want to note that we've observed large heterogeneity in telomere number per cell, likely because of aneuploidy, the presence of extrachromosomal telomere DNA, and the difference in the degree of clustering in these cells. The reader is referred to our previous publication for population plot: The figures here show representative images. For statistical analysis with more cells, please refer to Zhang et. al., 2020¹¹.

- A few typos were found: nucleic acids (line 50), vortex (line 113), optimum (lines 113, 118, 121 *2)

We corrected the typos.

Reviewer #2:

Manuscript Summary:

Dr. Zhang and colleagues show a protocol to study the telomere condensation generated by liquid-liquid phase separation, using chemically induced protein dimerization system; fusion of TMP and Halo (TNH).

This protocol has been written very carefully and provided many informative procedures for the colleagues in the field.

Major Concerns:

1. While using the TNH, a customized chemical reagent fused form of TMP and Halo, is the most important procedure in this protocol, no mention about how one can access this reagent. Alternatively, the author could introduce other commercially available chemicals.

The molecules are synthesized by David Chenoweth lab and will be available upon request. We added this information in the materials list.

2. There are several recent studies about ALT telomeres and PML phase separation (Zhang et al., 2019, Min et al., 2019, Loe et al., 2019) in addition to the author's recent work (Zhang et al., 2020), this reviewer suggests to refer these works as well.

We thank the reviewer for this comment. We expanded the introduction as following to include those reference: We use this tool to induce de novo promyelocytic leukemia (PML) nuclear body formation on telomeres in telomerase-negative cancer cells that use an alternative lengthening pathway (ALT) pathway for telomere maintenance^{13, 14}. PML nuclear bodies are membrane-less compartments involved in many nuclear processes^{15, 16} and are uniquely localized to ALT telomeres to form APBs, for ALT telomere-associated PML bodies^{17, 18}. Telomeres cluster within APBs, presumably to provide repair templates for homology-directed telomere DNA synthesis in ALT¹⁹. Indeed, telomere DNA synthesis has been detected in APBs and APBs play essential roles in enriching DNA repair factors on telomeres^{20, 21}. However, the mechanisms underlying APB assembly and telomere clustering within APBs were unknown. Since telomere proteins in ALT cells are uniquely modified by small ubiquitin-like modifier (SUMO)²², many APB components contain sumoylation sites^{22–25} and/or SUMO-interacting motifs (SIMs)^{26, 27} and SUMO-SIM interactions drive phase separation²⁸, we hypothesized that sumoylation on telomeres leads to enrichment of SUMO/SIM containing proteins and SUMO-SIM interactions between those proteins lead to phase separation. PML protein, which has three sumoylation sites and one SIM site, can be recruited to form APBs and coalescence of liquid APBs leads to telomeres clustering. To test this hypothesis, we used the chemical dimerization system to mimic sumoylation-induced APB formation by recruiting SIM to telomeres (Figure 2A)¹¹. GFP

is fused to Haloenzyme for visualization and to the telomere-binding protein TRF1 to anchor the dimerizer to telomeres. SIM was fused to eDHFR and mCherry. Kinetics of condensate formation and droplet fusion-induced telomere clustering is followed with live cell imaging. Phase separation is reversed by adding excess free TMP to compete with eDHFR binding. Immunofluorescence (IF) and fluorescence in situ hybridization (FISH) is also used. We observe that recruiting SIM enriches SUMO on telomeres and the induced condensates contain PML and therefore are APBs. Recruiting a SIM mutant that cannot interact with SUMO did not enrich SUMO on telomeres and did not induce phase separation, indicating that the fundamental driving force for APB condensation is SUMO-SIM interaction. Agreeing with this observation, polySUMO-polySIM polymers that fused to a TRF2 binding factor RAP1 can also induce APB formation³⁴. Compared to the polySUMO-polySIM fusion system where phase separation occurs as long as enough proteins are produced, the chemical dimerization approach presented here induces phase separation on demand and thus offers better temporal resolution to observe the kinetics of phase separation and telomere clustering process. In addition, this chemical dimerization system permits the recruitment of other proteins to assess their ability in inducing phase separation and telomere clustering. For example, a disordered protein recruited to telomeres can also form droplets and cluster telomeres without inducing APB formation, suggesting telomere clustering is independent of APB chemistry and only relies on APB liquid property¹¹.

Reviewer #3:

Manuscript Summary:

In the manuscript, Zhao et al described a method to induce protein condensates on telomeres through chemical dimerizer consisted of trimethoprim (TMP) and Halo ligand. Through the Halo ligand-Halo enzyme covalent interaction and TMP-eDHFR non-covalent interaction, the chemical dimerizer could induce the tethering of any protein (SIM as example) tagged with eDHFR to anchor proteins (TRF1 as example) tagged with Halo enzyme. The author provides detailed protocol for construction of cells, dimerization induction, living imaging, and fixed imaging of IF and FISH.

Minor Concerns:

Here, I have several points that the authors might want to consider.

1) How big are the tags used in this system? Whether it will affect the function of protein fused? Whether the size of the tags will affect the phase separation of the proteins studied.

Halo is 33 kD, eDHFR is around 28 kD, mCherry is 30 kD and GFP is 27 kD. Tags might affect the phase separation so we use controls such as SIM mutant to make sure that the phase behavior is sensitive to the mutations not the tags. We added this discussion in line 154.

2) In this protocol, 100 nM dimerizer is used. However, it seems pretty tricky to find a good concentration for other undefined system. As mentioned in the discussion, too low and too high dimerizer can't induce phase separation efficiently. Is there a range of the

suitable concentration? Can the authors provide more advice in the protocol for determining a suitable concentration for a new system?

We discussed how to determine a suitable concentration in line 204: NOTE: The concentration of dimerizers used affects dimerization efficiency and thus phase separation. The dimerizer concentration allowing maximum dimerization efficiency depends on cell type and anchor protein concentration, so it will need to be determined for different experiments. One simple way is to incubate cells expressing the anchor protein and mCherry-eDHFR (without fusing to the phase separating protein or fused to a non-phase separating mutant) and identify the dimerizer concentration at which the highest mCherry intensity at the anchor is achieved. A more systematic approach is to incubate cells expressing the anchor only with different concentrations of dimerizer and then with a Halo binding dye to help determine the dimerizer concentration at which the Halo binding dye intensity starts to plateau (i.e., all Halo-fused anchors are occupied by the dimerizer and no more left for the Halo binding dye)³¹.

We also discuss how dimerizer concentration can be used as a meaningful parameter for mapping phase diagram in line 526: Dimerizer concentration, along with the anchor DNA length and concentration of Halo-fused anchor protein, can be used to determine the critical concentration required for nucleating local phase separation. A systematic approach to vary those parameters (anchor DNA length, anchor protein concentration, phase separation protein concentration and dimerizer concentration) can help map a multi-dimensional phase diagram. However, if the interest is not in mapping phase diagram but forming chromatin associated-condensates like we demonstrated here, it is very easy to simply pick cells with bright Halo-GFP signal (larger anchor size) and cells with a wide range of brightness for mCherry-eDHFR (various phase separating protein concentration) to image with the dimerizer concentration for maximum dimerization determined in Protocol 2.3.

3) In the discussion (line 436-438), It's said "local condensation we depend on judging the physical properties of the foci, including size and intensity over time to verify phase separation". I don't think the increase of size and intensity can be easily used as evidence of phase separation. Any induced recruitment will have a process with gradual enrichment at certain loci, even without phase separation. Quantitative determination of fluorescent proteins is required to define whether there is extra enrichment of target proteins. Please give more comments about this point.

For the eDHFR fused prey proteins, the enrichment can be from both dimerization and phase separation, which can be difficult to differentiate. For the anchor protein, the intensity will increase only if the prey protein undergoes phase separation so it can be used to quickly judge whether there is phase separation. We expanded our discussion (line 542) to make it more clear: Different from global phase separation where droplets (bright mCherry foci labeling the phase separating protein) will emerge after phase separation, local condensation at genomic locations cannot be easily spotted by judging the presence of mCherry foci. This is because recruitment of the protein alone, without

phase separation, to genomic loci will result in formation of mCherry local foci. Phase separation occurs after recruitment, so mCherry foci continue to become bigger and brighter after initial recruitment. The phase separation induced enrichment can occur in GFP channel (the anchor protein) as well, due to the dimerization of the anchor protein to the phase separation protein. Therefore, change of physical properties (size and intensity) of the foci over time rather than the presence of foci should be used to judge phase separation. While it might be difficult to differentiate dimerization or phase separation-induced enrichment of mCherry foci, enrichment of the anchor protein only occurs if there is the prey protein condenses. Therefore, enrichment of anchor protein can be used to easily judge phase separation (Figure 3D). Photobleaching resulted from high laser power or long exposure time during imaging makes it more difficult to judge phase separation from live imaging and therefore should be avoided as much as possible by adjusting imaging conditions. Note that increase in foci intensity and size over time are characteristics of LLPS but cannot be used as the sole evidence for LLPS. In this case presented here, droplet fusion was used as evidence for the formation of liquid droplets, which may not occur for smaller number of anchors or less mobile anchors. Without droplet fusion, other methods such as diffusion of condensate components and sensitivity to small molecule perturbation can be used to further confirm condensate formation^{8,9,11}.

Reviewer #4:

Manuscript Summary:

In this article, Zhao et al. extend on their initial description of a newly developed/adapted live-cell assay to induce and analyze liquid-liquid phase separation (LLPS) at PML body-associated telomeres (ABPs) employing a chemical dimerization system (Zhang et al. MBoC 31:2048). Authors nicely describe in detail the procedure of this assay and hint to potential pitfalls and honestly indicate benefits and drawbacks of the approach in studying LLPS. With this protocol at hand, it will be straight forward for colleagues in the field of phase separation (in the nucleus) to establish the new approach in their own labs for their own projects. The study also describes potential further extensions to analyse LLPS at other subnuclear entities. Yet, a few minor points surfaced during the study of the manuscript which should be easily addressed by the authors:

Major Concerns:

none

Minor Concerns:

(1) line 106: Only U-2 OS (ALT-positive) cells were used in the current (and the previous study). Is SIM/TRF1-driven "artificial" LLPS also induced at telomeres in non-ALT cells (i.e. HeLa). This update will help colleagues to assess their own experiments.

We have data suggesting that SIM/TRF1 can also drive LLPS in HeLa cells and we are still analyzing the biological implications. We think this result is more appropriate to publish with the biological analysis later than in this protocol.

(2) line 162: "till" should be "until"

We corrected the error.

(3) line 173. Is "100 nM" the final concentration in the dish? Please clarify.

Yes, it's final concentration. We changed text to make it clear: Dilute dimerizer with growth medium to reach a final concentration of 100 nM.

(4) line 21: which mounting medium was used?

We use VECTASHIELD Antifade Mounting Medium. We added this information to the material list.

(5) line 251: what does ND acquisition mean?

ND acquisition is an dialog box in the image acquisition software (Elements) that allows us to define x,y,z and wavelength information. We changed our description to be less specific to the software: Find around 20 cells, memorize each position with x,y,z information and set up parameters for time lapse imaging with 0.5 μ m spacing for a total of 8 μ m in Z and 5 minute time interval for 2-4 hours for both GFP and mCherry channels.

(6) line 253, 282f: "Use 30% of 594 nm and 50% of 488 nm power intensity..." These values may be different for other than the Nikon (Spinning Disc) Confocal used here.

We added the laser power: The output power of laser units is 20 mW.

(7) Banani et al. used several SIM sequences, SIMs and mutated SIMS from which parent protein(s) were used here?

We added this formation to line 142: SIM is from PIASx²⁸. SIM sequence is AAAGTCGATGTAATTGACTTAACGATCGAATCTAGCAGCGATGAAGAAGAAGATCCACCGGCTAAACGT . SIM mutant is generated by mutating SIM amino acids VIDL to VADA²⁸, and the sequence is AAAGTCGATGTAGCCGACGCCACGATCGAATCTAGCAGCGATGAAGAAGAAGATCCACCGGCTAAACGT.

(8) line 361: the majority

We corrected this error.

(9) line 365 and additional lines: the word "diffusive" is not entirely correct here, better use "diffusely localized" or "homogenouosly distributed"

We changed to 'diffusely localized'.

(10) line 390: is "100 μ m" the final concentration? Please clarify.

Yes, it's final concentration. We changed text to make it clear: after adding 100 nM dimerizer (final concentration).

(11) The order of Figure description is different from the order of the figures (i.e. legend of Fig. 4 fits to Fig. 1), requires re-ordering.

We double checked the legends and figures to make sure they match.